A REVIEW OF AVHRR-BASED ACTIVE FIRE DETECTION ALGORITHMS: PRINCIPLES, LIMITATIONS, AND RECOMMENDATIONS

ZHANQING LI[1*], YORAM J. KAUFMAN[2], CHARLES ICHOKU[2], ROBERT FRASER[1], ALEX TRISHCHENKO[1], LOUIS GIGLIO[2], JI-ZHONG JIN[1] and XINWEN YU[1**]

[1]Canada Centre for Remote Sensing, Ottawa, Canada; [2]NASA Goddard Space Flight Center, Greenbelt, MD, USA

Abstract

As an important agent of climate change and major disturbance to ecosystems, fire is drawing increased attention from both scientists and the general public alike. Remote sensing plays an important role in obtaining quick and complete information on the occurrence and development of fires. There are currently dozens of algorithms that use different satellite sensors to detect and monitor fire activity around the world. This paper provides an overview of various Advanced Very High Resolution Radiometer (AVHRR)-based algorithms for detecting active burning in three general categories: single channel threshold algorithms, multi-channel threshold algorithms, and spatial contextual algorithms. Emphasis of the discussion is placed on their physical principles, merits, and limitations, as well as on areas of potential improvement. Recommendations are made to address some outstanding issues, such as cloud cover, surface reflection, and threshold setting. Five fire detection algorithms (IGBP, MODIS/AVHRR, ESA, CCRS, and Giglio *et al.*, 1999) are compared by applying them across the Canadian boreal forest for a six-month period and comparing cumulative fire pixels with a ground-truth data set. While fire detection algorithms are generally considered to be mature relative to algorithms for mapping burned areas, the performance of the algorithms under evaluation differs drastically, some producing considerable commission and omission errors. This implies that the hot spot detection algorithms are not robust enough for global operational use, and no single-sensor algorithm is optimal to generate global fire products. Suggestions are made to further explore the potential offered by both existing and future sensors that would help improve the performance of fire detection algorithms.

Introduction

Biomass burning has tremendous impact on the Earth's ecosystems and climate, for it drastically alters the landscape and vegetation patterns and emits large amounts of greenhouse gases and aerosol particles (Crutzen *et al.*, 1979; Crutzen and Andreae,

* now at: Department of Meteorology and ESSIC, University of Maryland, College Park, MD, USA
** now at: China Meteorological Administration, Beijing, P.R. China
Corresponding author: Dr. Z. Li, Dept. of Meteorology and ESSIC, University of Maryland, 2335 Computer and Space Sciences Building, College Park, MD 20742-2425, USA. Email: zli@atmos.umd.edu

Global and Regional Vegetation Fire Monitoring from Space: Planning a Coordinated International Effort, pp. 199–225
edited by F.J. Ahern, J.G. Goldammer and C.O. Justice

1990; Kaufman *et al.*, 1998a). Smoke aerosols may interact with cloud droplets (Kaufman and Fraser, 1997) and alter considerably the Earth's radiation budget (Li *et al.*, 1995,1998). Assessment and understanding of the wide-reaching and long-lasting effects of fires on the environment and climate entails a good knowledge of the spatial distribution and temporal variation of fire activity on a global scale. This may be achieved only through the use of remote sensing technologies, which provide an efficient and economical means of acquiring fire information over large areas on a routine basis, despite various limitations and shortcomings (Justice *et al.*, 1993; Setzer and Malingreau, 1996).

Several international programs have been established towards the goal of gaining complete information on fire activity around the world using satellite sensors. These include the International Geosphere Biosphere Program, Data and Information System's (IGBP-DIS) Global Fire Product initiative (Justice and Malingreau, 1993,1996), the World Fire Web, the ASTR World Fire Atlas (Arino and Rosaz, 1999), the MODIS Fire Product (Kaufman *et al.*, 1998a), and many other national and regional fire programs, as summarized in Grégoire *et al.* (this volume). These activities are among those endorsed by the Global Observation of Forest Cover program (Ahern *et al.*, 1998). The overall objective of GOFC is to improve our understanding of the impact of forest dynamics and forest fires on the global carbon budget, and to provide resource managers and decision makers with improved information about forest changes at continental to global scales. Since forest fires affect both forest dynamics and the carbon budget, monitoring and mapping forest fire is a major component of GOFC.

GOFC has two immediate requirements: near-real-time detection and monitoring of fires during the fire season; and post-fire season mapping of the burned areas.

These requirements respond to the needs of three fire user groups: the global change research community, policy and decision-makers, and fire managers (Ahern, *et al.*, this volume). Specific needs for fire information are diverse among these groups. For active fire detection, the main difference in the need for fire information lies in the promptness of information delivery, with fire managers and climate research community being the most and least demanding user groups, respectively. The speed of obtaining and disseminating fire information is currently dictated, to a large extent, by the fire monitoring systems that are reviewed in a separate paper in this book (Grégoire *et al.*, this volume). The accuracy of fire information is a common concern for all user groups that is determined primarily by fire detection algorithms, which are the subject of this paper. The accuracy is measured in terms of levels of both commission and omission errors and the location of fires detected that should be well defined and documented.

Remote sensing of fires has been achieved using a variety of space-borne systems/sensors. The most widely used sensor for long-term and large-scale fire monitoring is the Advanced Very High Resolution Radiometer (AVHRR) aboard the National Oceanic and Atmospheric Administration's (NOAA) polar orbiting

satellites (Flannigan and Vonder Haar, 1986; Kaufman *et al.*, 1990; Arino and Mellinotte, 1998; Justice *et al.*, 1996; Li *et al.*, 1997). Measurements from many other satellites have also been employed, such as GOES (Menzel *et al.*, 1991; Prins and Menzel, 1994), Landsat (Chuvieco and Congalton, 1988), DMSP (Cahoon *et al.*, 1992), ERS/ATSR (Arino and Rosaz, 1999), and in the recently launched Terra/MODIS (Kaufman *et al.*, 1998a). Each of the instruments has unique advantages and limitations for fire monitoring. For example, GOES offers frequent diurnal sampling (up to every 15 minutes), allowing a close surveillance of fire development, but at the expense of relatively poor spatial resolution (4 km or coarser) and limited coverage. In contrast, Landsat provides much more detailed information on the spatial distribution of individual fires, but suffers from an infrequent revisit (once every 16 days) and very small geographic coverage. It appears that AVHRR aboard NOAA satellites provides a reasonable trade-off between spatial and temporal coverage for global monitoring, with a variety of spectral bands. In addition, the long history of observation and well-understood sensor characteristics make AVHRR the workhorse for many GOFC programs. For example, AVHRR data have been employed to generate the first global fire product for the period April 1992-December 1993 under the IGBP-DIS fire initiative (Dwyer *et al.*, 1998), and are being used to produce a near real-time global fire data set under the WFW. Reconstruction of fire history over all of North America is also under way by US and Canadian scientists under NASA's Land Use and Land Cover Change Program, a US contribution to GOFC. A more ideal instrument for fire monitoring is MODIS (on board the Terra satellite launched in December 1999), which includes special channels tailored to fire monitoring (Kaufman *et al.*, 1998a). However, MODIS has yet to provide a long-term record of data.

In light of their unique and important role, AVHRR-based fire detection algorithms are the focus of this paper. Algorithms using data from other sensors are discussed in separate papers in this book. A modified MODIS algorithm adapted to AVHRR data is also discussed, due to its similarity to the AVHRR algorithms. The following section describes the characteristics of AVHRR sensors. This chapter is structured as follows:

- a review of the characteristics of the AVHRR and MODIS sensors;
- a review of AVHRR-based fire detection algorithms in terms of their physical principles and limitations;
- an evaluation of the efficiency and performance of five commonly used algorithms by applying them to the Canadian boreal forest as a demonstration, which may not be valid for other ecosystems;
- general and specific recommendations as to how the algorithms may be improved;
- summary and conclusions.

Characteristics of sensors

To better understand fire detection algorithms, the characteristics of NOAA/AVHRR, as well as of EOS/MODIS, are described first. NOAA/AVHRR has two major advantages for fire monitoring. Firstly, the instrument provides daily coverage of the entire planet at a moderate resolution (~1 km), which is critical for operational global fire monitoring. Secondly, it has wide spectral coverage comprising the visible (channel 1, 0.63 ìm), near-infrared (channel 2, 0.83 ìm), mid-infrared (channel 3, 3.75 ìm), and thermal (channel 4-5, 10-12 ìm) wavebands. All channels are sensitive to certain attributes of fire, but contain different information (Li *et al.*, 1997). Smoke is more discernible in the visible channel, which has been employed to estimate fire smoke and trace gas emissions (Kaufman *et al.*, 1994). However, due to the similar appearance of smoke and clouds in this channel, identification of smoke is better achieved with other AVHRR channels (Li *et al.*, 2000a). Burned area can be assessed from reflectance differences between the visible and NIR channels (Kasischke *et al.*, 1993; Razafimpanilo *et al.*, 1995; Li *et al.*, 2000b; Fraser *et al.*, 2000), or from indices derived from the NIR/MIR spectral domain (Pereira, 1999; Barbosa *et al.*, 1999). In principle, the size and temperature of sub-pixel fires may be determined from the thermal radiance in two infrared channels (channel 3 and channel 4) for a uniform background (Dozier, 1981), if the sensor is not saturated and the signal is significant in both channels. In practice, this has often proven to be a difficult task. For example, deforestation fires in South America that are detected by AVHRR increase the signal at 10 μm on average only by 1.5 K, which is within the background variability in this channel (Kaufman *et al.*, 1990). The essence of fire detection lies in significantly enhanced radiance emitted in the mid-infrared region (channel 3) for typical fire temperatures, as governed by the Planck function. The mid-infrared channel is thus most useful for fire detection. It is highly sensitive to the presence of fires, which also poses a problem for fire detection. A very small fire within the 1-km pixel can easily saturate the channel. For example, a fire with a temperature of 1000 K located within a non-reflective background of 300 K, needs only be 13 × 13 m to saturate the 3.75 μm channel (Kaufman *et al.*, 1990; Robinson, 1991; Belward *et al.*, 1993). To overcome the problem, channel 4 is often used in combination with channel 3. For moderate resolution satellite data like AVHRR, fires usually have varying temperature within the pixel, rendering unusually large differences in brightness temperature between the two channels.

The MODIS fire detection algorithms are based on those developed for AVHRR, but bring some new capability to the remote sensing arena. In the MODIS design, the 3.75 μm channel was shifted to 3.95 μm to avoid variable water vapor absorption and to reduce reflected solar radiation by 40% (Kaufman *et al.*, 1998a). MODIS visible and near IR channels (0.66 and 0.86 μm) both have a resolution of 250 m, which is advantageous for more accurate remote sensing of vegetation and burn scars. MODIS has a 1.65 μm channel (with a resolution of 500 m) that

has been shown to be very sensitive to burn scars (Kaufman *et al.*, 1998b; Eva and Lambin, 1998). MODIS smoke detection employs the blue (0.41 and 0.47 μm) and mid-IR (2.1 μm) channels in addition to the AVHRR red channel (0.66 μm) for better detection and discrimination of smoke from soil dust (Kaufman *et al.*, 1997; Chu *et al.*, 1998).

Review of algorithms: principles and limitations

Given that AVHRR fire detection algorithms have been reviewed in several previous papers (Robinson 1991; Justice *et al.*, 1993; Setzer and Malingreau 1996; Martin *et al.*, 1999), the overview given here is brief and focuses more on the physical principles. Similar to the recent classification by Martin *et al.* (1999), the majority of AVHRR-based fire detection algorithms may be classified into three categories: *1.* single channel threshold algorithms based on channel 3; *2.* multi-channel threshold algorithms; and *3.* contextual algorithms that compare the potential fire pixel with the thermal properties of the background. Note that the single channel and multi-channel threshold algorithms are basically fixed threshold methods, while the contextual ones have variable values of thresholds. There may be a few other types of fire detection algorithms using AVHRR data that are not typical enough to be reviewed here, such as the raw digital count method used operationally in Brazil (Setzer and Pereira, 1991a; Pereira and Setzer, 1993).

Single-channel threshold algorithms

The single-channel threshold algorithms rely only on AVHRR's mid-infrared channel, *i.e.*, channel 3 centered around 3.75 μm. According to the Planck function, emission of thermal radiative energy in the spectral region of channel 3 reaches peak values for typical fire temperatures ranging from 500 K for smouldering fires to over 1000 K for flaming fires (Fig. 1). However, since AVHRR was not designed for fire monitoring, it is saturated at a brightness temperature of 320-331 K (Robinson, 1991), well below the fire temperature. For example, on a background of 300 K, a hot object at 1000 K that occupies only 0.02% of the pixel area can raise the pixel's brightness temperature at 3.75 μm to 324 K. Nevertheless, a non-fire target rarely reaches the saturation point, barring strong reflection of solar radiation due to clouds or bright land. Therefore, the saturated channel 3 is still useful for detecting the presence of fires especially for relatively cool environments and/or regions with low solar reflectivity (Muirhead and Cracknell, 1985; Malingreau and Tucker, 1988; Setzer and Pereira, 1991b, 1992). The single-channel threshold algorithm was also applied to other sensors such as the ATSR (Arino and Rosaz, 1999). Single-channel thresholding is most useful for the evening satellite overpasses, where the contribution from reflected sunlight is minimal (Malingreau 1990; Langaas, 1992).

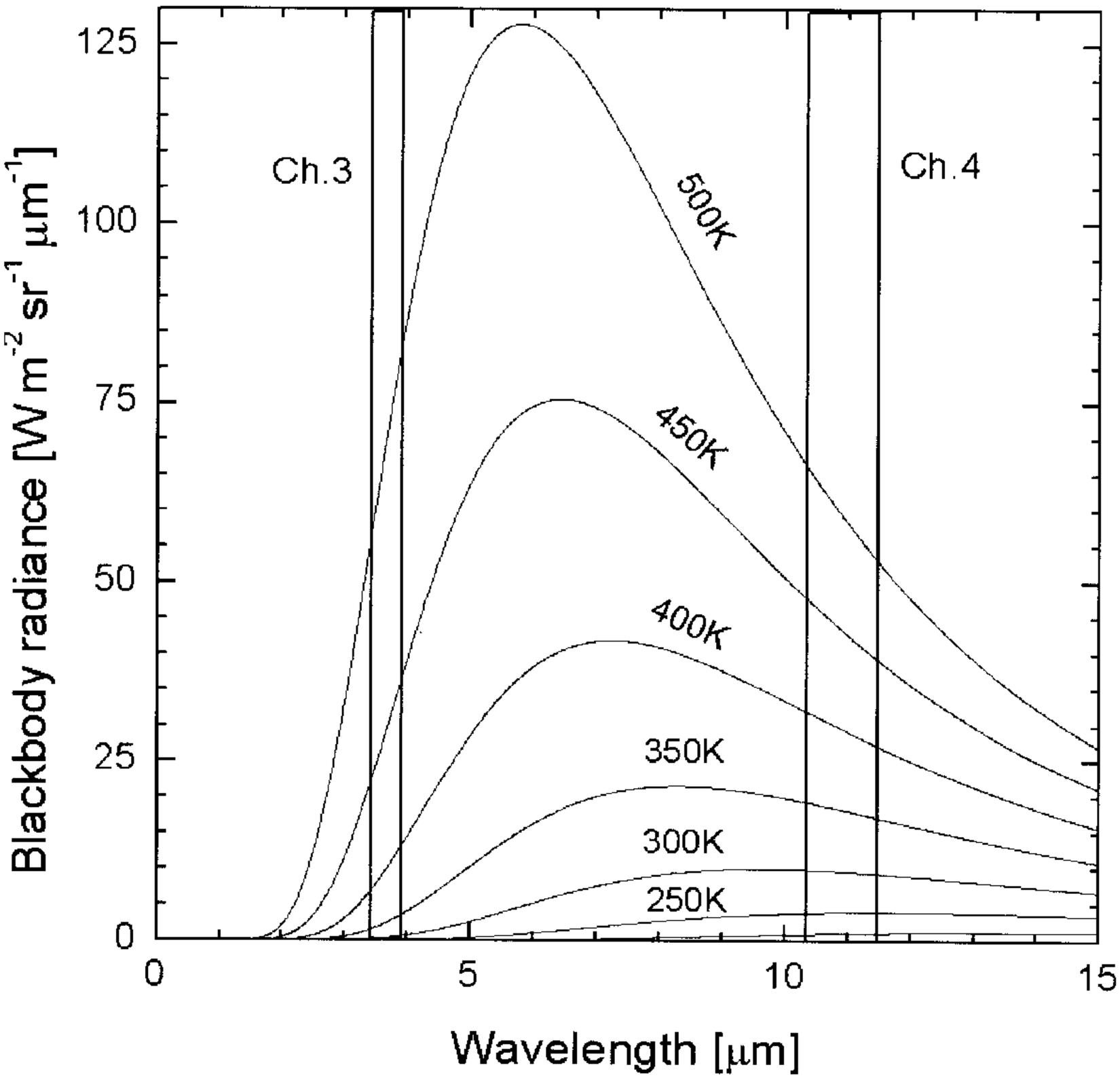

Fig. 1. Plank function and the locations of AVHRR channels 3 and 4 (modified from Matson *et al.*, 1987)

The most challenging task in using channel 3 to detect fires during daytime is to account for the influence of solar reflection from cloud and bright surfaces within the limits dictated by the low saturation of channel 3. For example, a soil surface with a temperature of 300 K and a reflectance of 0.28 can saturate the 3.75 μm channel, even when no fire is present (Giglio *et al.*, 1999). While fire reflectivity (= 1-emissivity) in channel 3 is very low (almost zero) for fires and decreases with increasing flame depth and intensity (Vines, 1981; Robinson, 1991), the reflectivity of other scene types is not negligible and quite variable (Salisbury and D'Aria, 1994; Giglio *et al.*, 1999). For barren soils, reflectivity in channel 3 ranges from 0.13 to more than 0.4, according to the survey of Setzer and Malingreau (1996) based on the studies of Hovis (1966) and Suits (1989). The relative contribution of this component to the total channel 3 radiance is demonstrated in Figure 2. It is seen that the reflection of solar radiation plays an increasing role as surface temperature decreases. Solar reflection depends mainly on the amount of incident solar radiation and the albedo. For $\mu_o = 0.8$ albedos above 40% can cause channel 3 to saturate, where μ_o = cos (solar zenith angle). Albedos above 20% can confuse most fire detection algorithms. If the albedo is 5%, solar reflection can never cause saturation of channel 3 without the presence of a fire. This

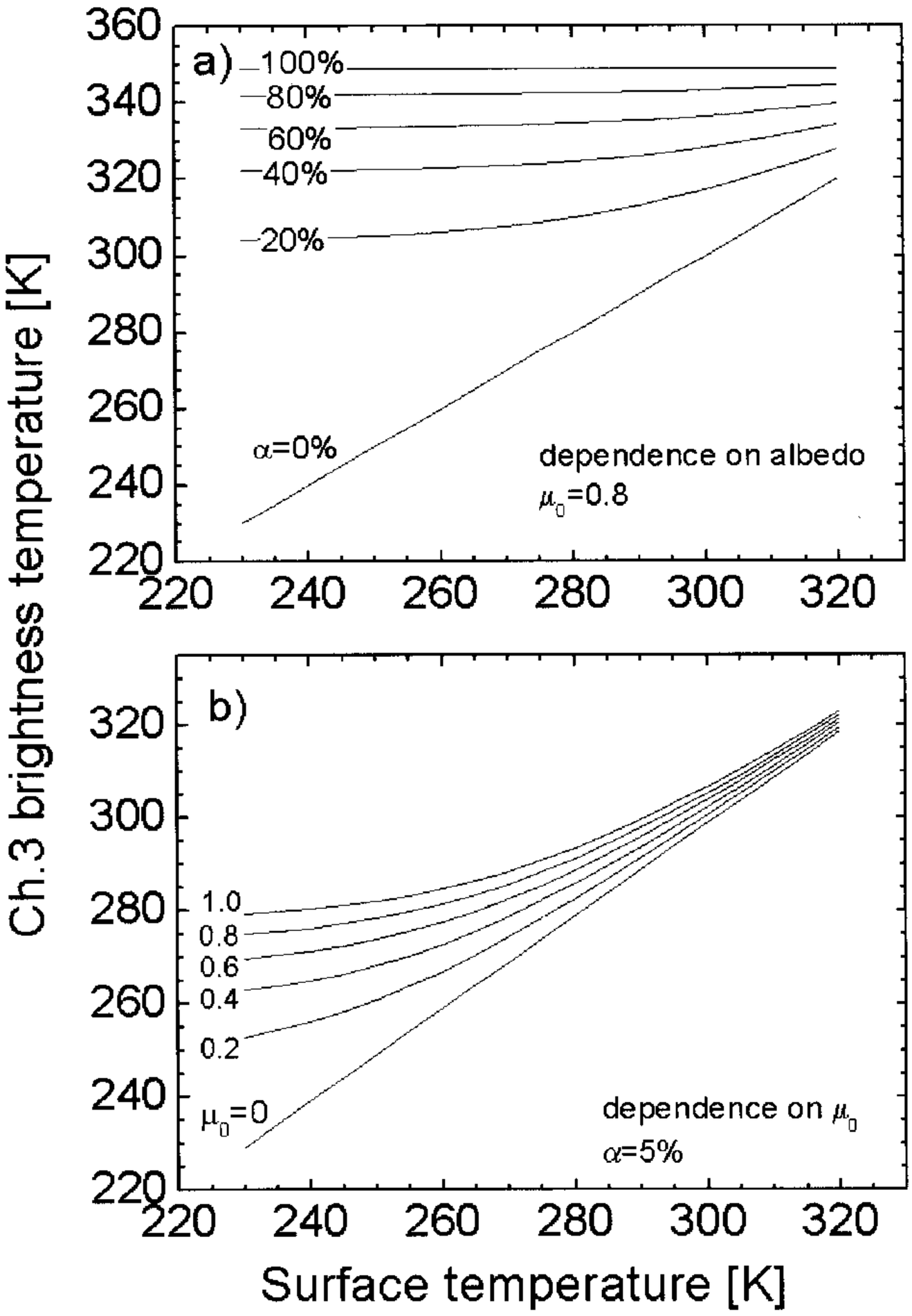

Fig. 2. Relationship between AVHRR channel 3 brightness temperature and surface temperature with varying contributions of solar reflection. The brightness temperatures are inverted from radiances using the Planck function with the brightness temperature as a parameter, where the radiance is computed from

$R_3 = \alpha S_0 \mu_0/\pi + (1-\alpha) B(\lambda_3,T_s)$,

where R_3 is the radiance in channel 3, S_0 is the solar constant in channel 3, μ_0 is the cosine of the solar zenith angle, α is the surface albedo, $B(\lambda_3,T_s)$ is the Planck function, λ_3 is the effective wavelength of channel 3, and T_s is the surface temperature. Atmospheric attenuation is neglected. The upper and lower panels show the influence of the albedo and solar zenith angle.

is the case for the majority of vegetated land, especially forest, which usually has a channel 3 albedo below 5% (Kaufman and Remer, 1994; Giglio *et al.*, 1999; Flannigan and Vonder Haar, 1986). For other types of surface, the albedo in channel 3 is large and more variable, ranging from 0.14 for winter grassland and tropical savanna to 0.24 for desert (Giglio *et al.*, 1999). The albedo of clouds can be even larger and more variable. In view of the above concerns, two recommendations are made to improve the performance of fire detection algorithms intended for application across a range of land cover types:

- screening of bright objects (*e.g.*, cloud, bare surfaces) is applied prior to the use of channel 3 to identify potential fires in order to increase the effectiveness of channel 3 thresholding;
- the channel 3 threshold should vary according to both land cover type, or more precisely channel 3 albedo, and the amount of incoming solar radiation (*e.g.*, use solar zenith angle as a proxy variable).

These recommendations are particularly applicable for detecting fires that are not hot or large enough to cause saturation in channel 3.

Multi-channel threshold algorithms

To overcome some of the difficulties with single-channel fire detection, multi-channel threshold algorithms were introduced. The majority of the multi-channel threshold algorithms consist of three basic steps (Kaufman *et al.*, 1990): *1.* use channel 3 to identify all potential fires; *2.* use thermal channel 4 to eliminate clouds; and *3.* use the difference between brightness temperature in channels 3 and 4 to isolate fires from warm background. Note that these improvements do not correct for the possible presence of reflective surfaces. The multi-channel threshold algorithms were mainly used for regional or even continental applications. So far, they have been applied to detect fires in various biomes such as tropical forest (Kaufman *et al.*, 1990; Belward *et al.*, 1994), savanna fires in West Africa (Langaas, 1993; Kennedy *et al.*, 1994; Franca *et al.*, 1995), and boreal forests (Cahoon *et al.*, 1991,1994; Li *et al.*, 1997,2000c). For each application, thresholds were specifically tuned to cope with unique environmental and fire conditions. In addition to the three basic tests, additional tests may also be applied, in particular for coping with reflective surfaces and different types of clouds. Note that channel 4 is efficient for detecting high cloud decks with cold cloud tops, but it is not effective for removing low clouds which have little thermal contrast with the surface, or residual sub-pixel clouds. Channel 1 visible reflectance measurements have been used to remove low cloud and bright surfaces (Kennedy *et al.*, 1994; Arino, 1998). However, among all the AVHRR channels, the visible channel is most susceptible to fire smoke that often accompanies fires, unless it is blown away from fires by strong wind. The channel 2 NIR observation was also used for the same purpose (Li *et al.*, 2000c), which is also affected by smoke but to a substantially lesser degree. Another advantage of using channel 2 is that vegetation albedo diminishes drastically after burning, leaving more contrast with green vegetation. The difference between brightness temperature in channel 4 and 5 (T4-T5) is useful to remove thin cirrus clouds (Inoue, 1987; Franca *et al.*, 1995; Li *et al.*, 1997,2000c), while the spatial coherence technique proposed by Coakley and Bretherton (1982) was used to exclude sub-pixel clouds (Flannigan and Vonder Haar, 1986).

Among these tests, the T3-T4 test is most efficient in removing false fires, as is shown in later analyses. The test has thus been adopted in all multi-channel

threshold algorithms. The common notion is that fire pixels have significantly larger values of T3-T4 than non-burned background. However, the physical basis behind this test is considerably more complex. In principle, four contributing factors could create the T3-T4 difference: *1.* unequal atmospheric effects; *2.* unequal emissivities; *3.* solar reflection in channel 3; and *4.* non-uniform fire scenes. Unequal atmospheric effects in the two channels contribute to a difference between T3 and T4, as the transmittance in the two channels is different (Fig. 3). In general, the atmosphere is more transparent in channel 3 than in channel 4, with average transmittances approximately 0.9 and 0.75 in channels 3 and 4, respectively. On the other hand, atmospheric emission is proportional to the transmission. These offsetting effects of the atmosphere dampen the difference in the inverted brightness temperature. Figure 4 shows the relation between top of atmosphere brightness temperatures (T3, T4) and surface blackbody temperature (T). The results were obtained by using the Planck function and a MODTRAN code (Anderson *et al.*, 1986) for a subarctic model summer atmosphere. It follows that *(a)* both T3 and T4 vary linearly with T, and *(b)* T3-T, T4-T and T3-T4 are usually small for ordinary terrestrial surfaces and increase with T. For T3-T4 to reach a difference of 10 K (a typical threshold used in fire detection algorithms), T needs to be above 370 K and T3 above 363 K. Since channel 3 becomes saturated around 325 K, large differences in T3-T4 could not be incurred

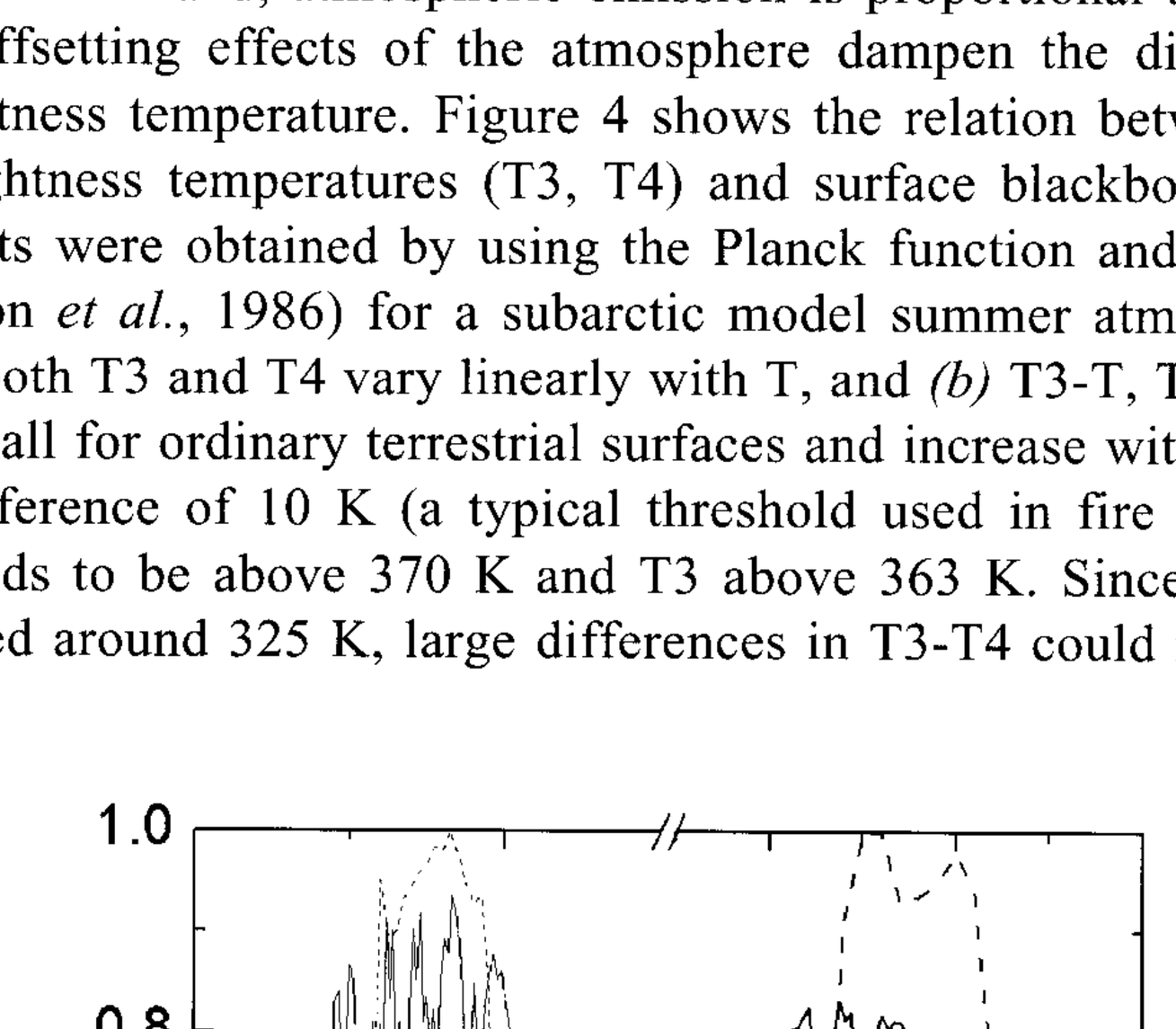

Fig. 3. Atmospheric transmittances (solid curves) in the spectral regions of AVHRR channels 3 and 4 computed by MODTRAN 3.7 for the sub-Arctic summer atmosphere. The radiometer's spectral response functions are also shown.

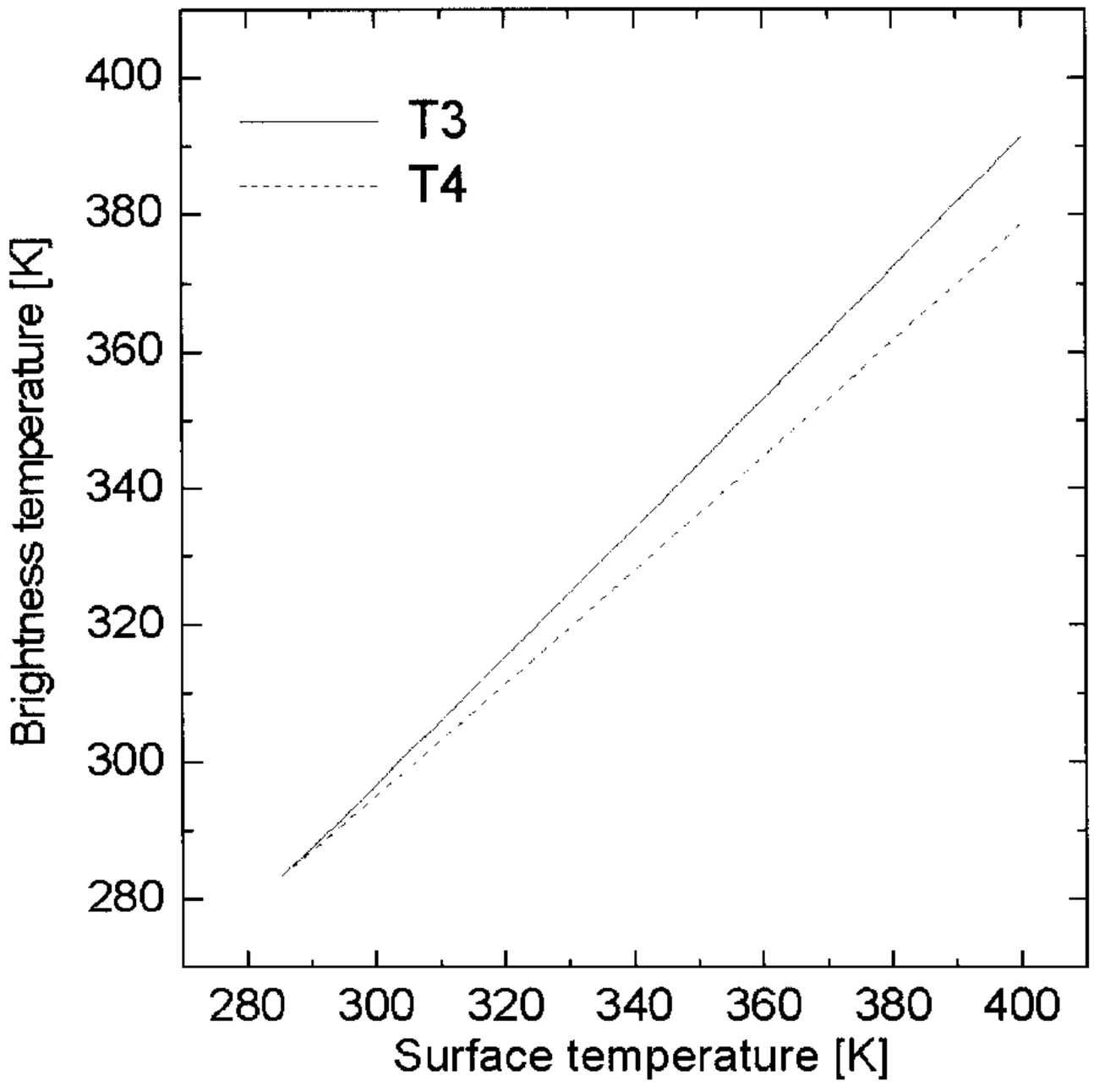

Fig. 4. Relationships between the brightness temperature at the top of the atmosphere and the surface temperature in AVHRR channels 3 and 4. Atmospheric effects are accounted for by the MODTRAN 3.7 code that computes atmospheric attenuation, due to absorption and enhancement due to emission.

by a uniform, hot pixel. On the contrary, hot fires may induce negative values for T3-T4, as the saturation temperature for channel 4 is typically somewhat higher (~330 K). The maximum T3-T4 reachable before T3 saturation (say 325 K) is about 4-5 K. Different emissivities in channels 3 and 4 contribute to the difference in T3-T4, but the contribution is usually minor. Because deserts have quite different emissivities in channels 3 and 4 (0.76 and 0.97, respectively), they can produce negative T3-T4. Moreover, there is no evidence showing that fires have larger differences in emissivities between channels 3 and 4 than background scenes. Solar reflection in channel 3 can cause large T3-T4, but this introduces false alarms rather than helps remove them.

The driving factor causing large T3-T4 differences is the inhomogeneous temperature fields containing fires, as simulated by Dozier (1981) and Kaufman *et al.* (1998a); and measured by Kaufman *et al.* (1998b). Because of the nonlinear dependence of radiance on temperature, the more heterogeneous the temperature field, the larger the difference in T3-T4 is. This forms the basis for removing false fires when using coarse resolution satellite data such as the 1-km AVHRR data. This test would not be as effective for fine resolution data such as LANDSAT/TM, where fires would frequently cover a large proportion of a pixel. Figure 5 shows the simulation results of T3-T4 against the fraction of fire within a pixel. Only two different temperatures within a pixel are considered: a cool background (300 K) and a hot fire whose temperature enhancement is indicated in the plot.

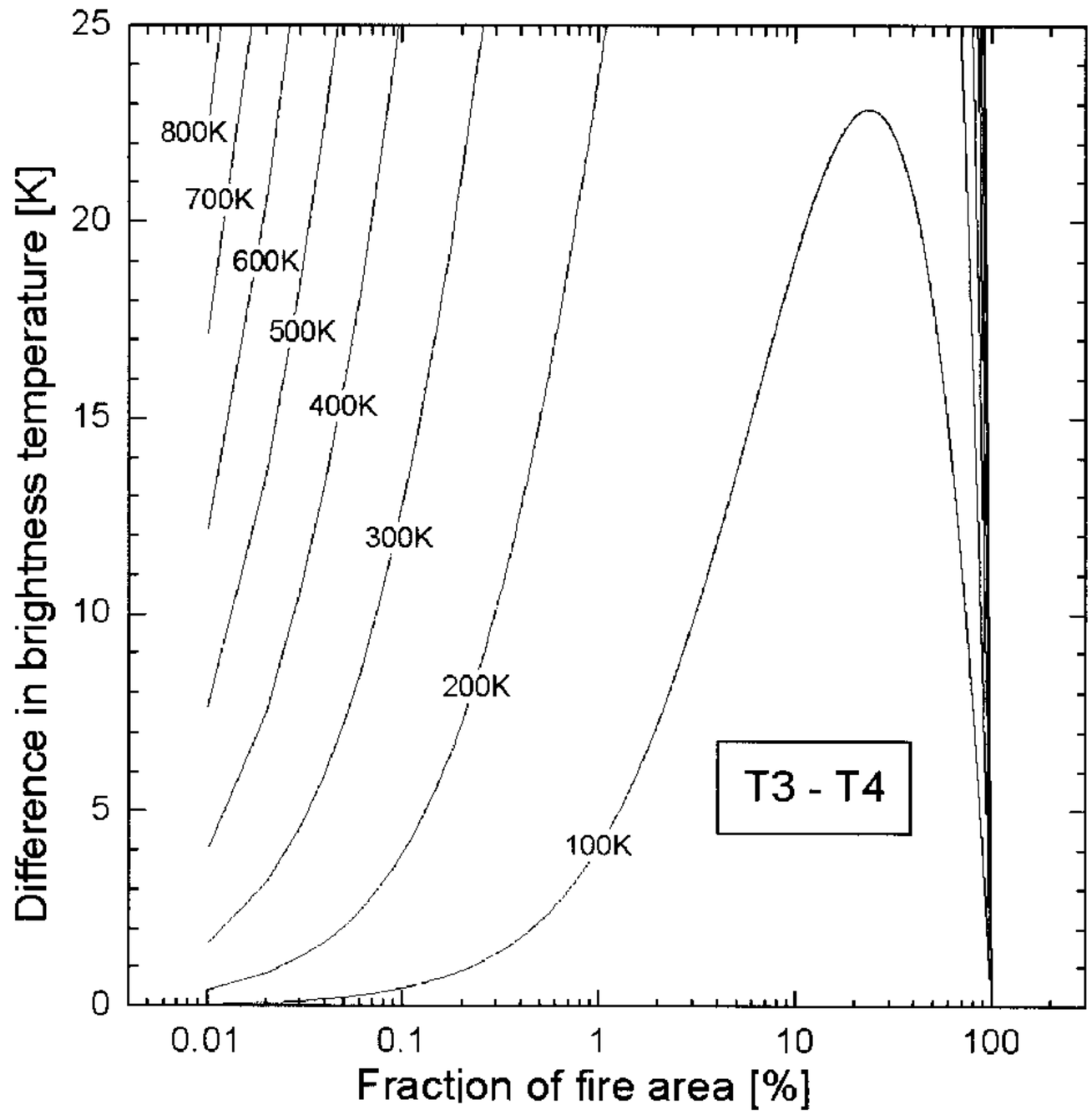

Fig. 5. Difference between AVHRR channels 3 and 4 TOA brightness temperatures as a function of the fraction of a fire whose temperature exceeds the background temperature by an amount ranging from 100-800 K.

T3-T4 is found to reach maximum values for a very small fraction of fire area. The hotter the fire, the smaller the fraction required to reach maximum T3-T4. As the fire fraction increases, T3-T4 decreases. For fires whose temperature exceeds surface temperature by more than 500 K (rather typical), the T3-T4 difference reaches the maximum when the fire fraction is well below 0.1%. If the entire pixel is burning with a uniform temperature, the difference in T3 and T4 vanishes! As such, the use of the T3-T4 difference does not help the detection of large uniform fires.

Giglio *et al.* (1999) simulated the probability of detection by AVHRR fire algorithms, and found that they all miss fires of large fractions ranging from as low as less than 1-10%, depending on fire temperature and satellite viewing zenith angle (Fig. 6). Use of AVHRR measurements made at large viewing zenith angles reduces this problem, as the fire fraction decreases with increasing pixel size, while there is a concomitant decrease in the probability of detecting small fires. Fortunately, it is rare for a fire to occupy a large proportion of an AVHRR pixel with uniform temperature, as the fire frontier is usually quite narrow. Besides, a fire field usually exhibits rather diverse temperatures that may vary by several hundred degrees (Robinson, 1991). In the case of large and relative uniform fires, channel 4 could be used to identify fires by setting a higher threshold, or by examining relative spatial contrast of T4 with respect to its surrounding pixels. For such fires, the commonly used T3 and T3-T4 tests are no longer

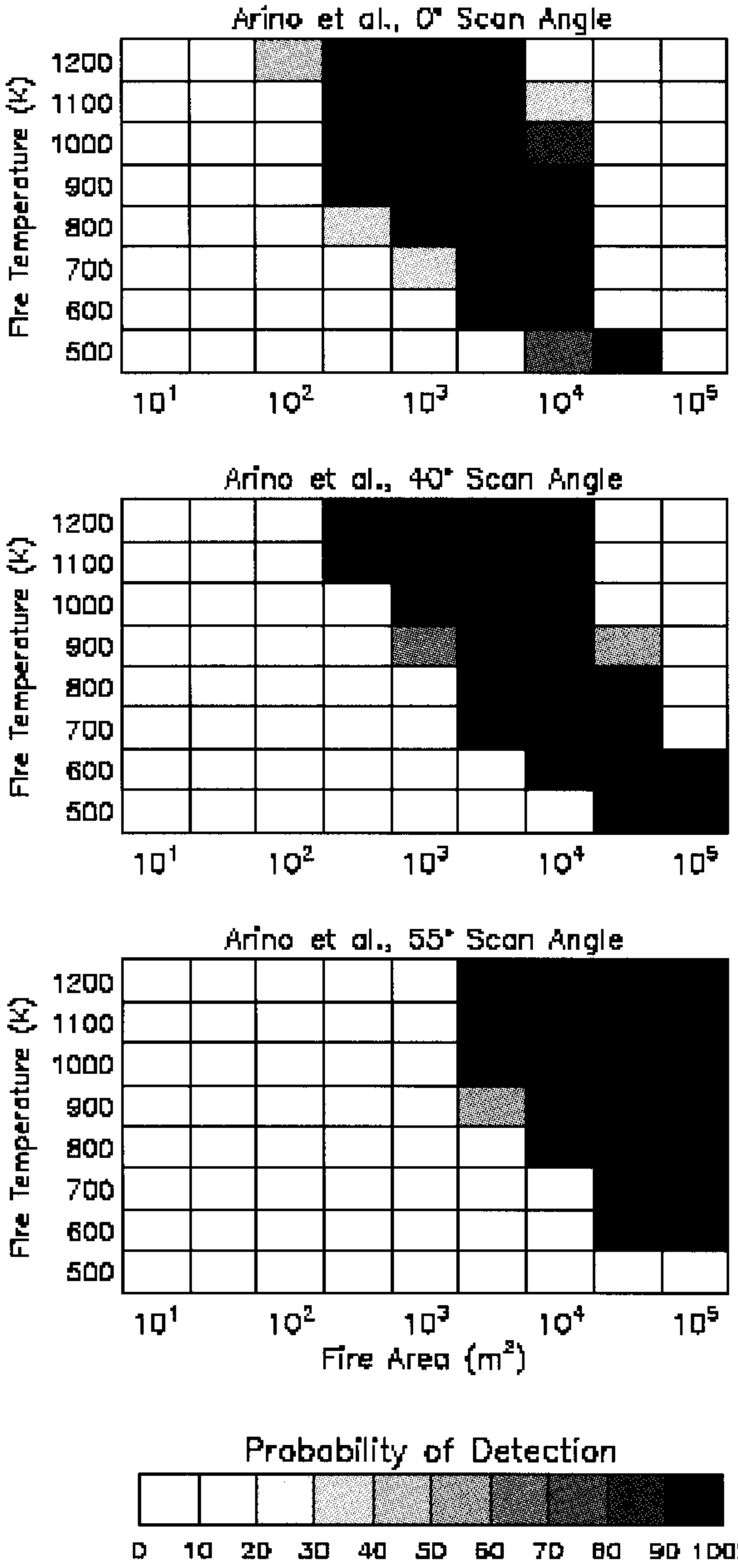

Fig. 6. Fire detection envelop at scan angles of *(a)* 0°, *(b)* 40°, and *(c)* 55° using the ESA algorithm (Arino and Mellinotte 1998) for fires in the tropical rain forest biome (from Giglio *et al.*, 1999).

effective. This problem will be largely eliminated with MODIS fire detection, since the 3.95 μm channel (replacing the AVHRR 3.75 μm channel) is not easily saturated by a fire, and a simple absolute threshold at 3.95 will detect these large fires with no need for the T3-T4 difference threshold.

Contextual algorithms

To expand the utility of multi-channel algorithms, multi-channel contextual algorithms were proposed (Lee and Tag, 1990). They were first explored by the IGBP DIS fire working group (Justice and Malingreau, 1993) using AVHRR data, and by Prins (1992) using GOES data. The approach was further employed for global and regional fire monitoring (Justice and Malingreau, 1996; Eva and Flasse, 1996; Dwyer *et al.*, 1998), and is now used for the World Fire Web initiative (Grégoire *et al.*, this volume). Instead of using fixed thresholds throughout a study region, a contextual algorithm computes variable, pixel-specific thresholds. This involves two basic steps: initial setting of thresholds to identify potential fire pixels and then fine-tuning the thresholds to confirm fires among the potential fire pixels (Martin *et al.*, 1999). The tests in the first step are similar to the multi-channel threshold techniques except that the thresholds are more liberal to avoid missing real fires. The second step computes the mean and standard deviation of the threshold variables (*e.g.*, T3 and T3-T4, among others) from non-potential fire pixels surrounding a potential fire pixel. The window size for computing the means and standard deviations is set in a somewhat *ad-hoc* manner, varying typically from 3 × 3 pixels up to 21 × 21 (Flasse and Ceccato, 1996), until the number of qualified background pixels reaches a prespecified value (usually 25% or 3). After obtaining these statistics, they are used to redefine the thresholds to confirm a fire. Giglio *et al.* (1999) proposed different thresholds for marking initial potential fires and for confirming real fires. Examples of the threshold settings are presented in a later section. For regional application, there is an advantage to set the thresholds based on regional and seasonal varying surface properties, fuel type and amount, fire strength, etc. (Martin *et al.*, 1999; Chuvieco and Martin, 1994). For global application, a more conservative fire detection algorithm is sometimes desirable. Note that a conservative, global algorithm can be expected to miss many of the smaller fires in an attempt to reduce false fire detection. Therefore, such algorithms will be less useful for early fire detection and tactical response. However, these approaches detect the larger fires that are responsible for most of the biomass burning and climate impact. For example, Kaufman *et al.* (1998b) found that in Brazil, the MODIS algorithm was capable of detecting only 30-40% of the fires, but these fires are responsible for 80-99% of the burned biomass.

Evaluation and inter-comparison of algorithms and tests

So far, the discussion has been largely theoretical, while many fire detection algorithms were developed empirically. Both empirical and theoretical algorithms need to be validated thoroughly and extensively, so that the accuracy and limitations of resulting fire products are well documented. While many fire detection

algorithms have been proposed, few have been rigorously validated. In most cases, only cursory validations were conducted by comparing against fire smoke plumes. A handful of satellite-based fire studies (*e.g.*, Flannigan and Vonder Haar, 1986; Setzer and Pereira, 1991b; Setzer *et al.*, 1994; Rauste *et al.*, 1997; Li *et al.*, 1997,2000c) have performed validations using ground-truth information on actual fires. However, such ground-truth data are severely lacking in most parts of the world. Validation of fire detection algorithms thus remains an acute problem. Apart from validation against ground-truth data, algorithm inter-comparison is also helpful for gaining insight into the performance of the algorithms, at least regarding the consistency among the algorithms under study.

Canada is one of the few countries that maintains a relatively detailed and complete archive of forest fire distribution, allowing evaluation of satellite-based fire detection. In Canada, GIS-based fire polygons showing both the area and spatial distribution of forest fires are produced by provincial and terrestrial fire management agencies using airborne infrared mapping techniques. The Canadian Forest Service (CFS) gathers, compiles, and standardizes the digital fire information and distributes them in GIS format through a National Forestry Database. Such a nation-wide fire inventory data are available for many years. Only the end-of-season (cumulative) burned area polygon data for 1995 are examined here.

Efficiency of individual tests

Before evaluating the performance of fire detection algorithms, the efficiency of individual fire detection tests that are commonly used is examined. It follows from the above overview that fire detection algorithms exploit information from most of the AVHRR channels. However, these channels do not play equal roles. Li *et al.* (2000c) examined the relative efficiency of these channels/tests using their multi-threshold algorithm applied over the Canadian boreal forest. The efficiency is measured in terms of the numbers of false fires eliminated (NFF) and real fires retained (NTF) after each test, as is shown in Table 1.

Note that the real fires in the test data set were determined following visual inspections for smoke plumes, and were not confirmed using the CFS fire database. The statistics were derived over a 1000 × 1000 km^2 region in western Canada. It is clear that use of a channel 3 threshold alone produces a very high proportion of false fires. Although its threshold could be increased to reduce false fires, the number of real fires would also decrease concurrently. Fortunately, the use of series of tests can drastically lower the number of false fires by as much as 98%, but the number of real fires remains largely intact (~10% reduction). The most efficient test for removing false fires is the T3-T4 test, followed by tests based on R2 (reflectance at channel 2), land cover, etc. Except for the T3-T4 test, relative efficiencies for other tests depend partly on the sequence of implementing the tests. The T4 cloud test appears to be redundant here. However, had the test been applied prior to the R2 test, it would have been much more significant. For the

Table 1. Summary of the fire-detection tests and the statistics of their efficiency (after Li *et al.*, 2000c)

Test No.	*Description*	*Threshold*	*NTF*	*NFF*
1	Initial test	T3 > 315 K	12,569	168,168
2	Eliminate warm background	T3-T4 >14 K	12,569	48,855
3	Eliminate non-forest scenes	Land cover	12,569	30,511
4	Eliminate bright scenes	R2 < 0.22	12,442	5,665
5	Eliminate cloud edges or thin clouds	T4-T5>4.1 K T3-T4<19 K	11,307	2,673
6	Eliminate cold clouds	T4<260 K	11,307	2,673
7	Eliminate single fire pixels		11,160	1,828

NTF and NFF: numbers of true and false fires remaining after each step of the detection tests, respectively

boreal forest, the solar reflective channel shows better contrast than thermal channels between cloudy and clear scenes. It is worth noting that the output shown in Table 1 depends on the algorithm used and the region or season of application, but the conclusions concerning the T3 and T3-T4 may be valid in general. Such an analysis is useful in developing a fire detection algorithm and understanding its performance.

Evaluation and comparison of the performance of five algorithms

As a demonstration of the utility of inter-comparison exercises, five fire detection algorithms were applied to AVHRR data acquired across Canada. The results from these algorithms are compared to each other and also to the ground-truth data. The analysis serves: *1.* to characterize the performance of the algorithms in perspective; *2.* to check the magnitude of inconsistency among different algorithms; and *3.* to identify some common problems. Note that the results of the analysis may not be generalized, as they are for a specific ecological and geographical domain. The five algorithms under study include four designed for global applications and one for boreal forest (for details, see Table 2). The global algorithms include one used in generating the IGBP-DIS fire product (Malingreau and Justice, 1997), one designed for the MODIS (Kaufman *et al.*, 1998a,b), one employed at the European Space Agency (ESA) (Arino and Mellinotte, 1998), and one proposed by Giglio *et al.* (1999). The regional algorithm was developed and is operated at the Canada Center for Remote Sensing (CCRS) (Li *et al.*, 2000b). Two of the algorithms use fixed thresholds (CCRS and ESA) and three use contextual methods with variable thresholds (IGBP, MODIS/AVHRR, and Giglio *et al.*, 1999). All the objective tests in each of the algorithms as listed in Table 2 were implemented. In implementing the three contextual algorithms, the same cloud screening tests were applied following the IGBP, namely, $R1 + R2 \leq 1.2$, $T5 \geq 265$ K, $T5 \geq 285$ K OR $(R1+R2) \leq 0.8$. Pixels passing all these tests are

Table 2. Five fire detection algorithms tested over the Canadian boreal forest. Note that all statistics (av, ad, md, sd) refer to background pixels; all temperature values are expressed in degrees Kelvin (K); all thresholds given here refer to daytime data

Algorithm/description	*CCRS*	*ESA*	*IGBP*	*GIGLIO*	*MODIS/AVHRR*
Algorithm category and geographic applicability	fixed thresholds, regional (Canada)	fixed thresholds, global/regional	contextual, global	contextual, global	contextual, global
Potential fire detection			T_3>311 and T_{34}>8	T_3 >310 and T_{34}>6	T_3 ≥315 and T_{34}≥5
Background window size			3 × 3 to 15 × 15	5 × 5 to 21 × 21	3 × 3 to 21 × 21
Minimum number of pixels			Max(25% of pixels tested, 3)	Max(25% of pixels tested, 6)	Max(25% of pixels tested, 3)
Background selection			T_3≤311 or T_{34}≤8	T_3≤318 or T_{34}≤12	T_3≤320 or T_{34}<20
Actual fire detection with T_3 and/or T_4	T_3>315	T_3>320	Define: ξ_3= av(T_3)+2*sd(T_3)+3 ξ_{34}= Max{8, av(T_{34})+ 2*sd(T_{34})}	Define: ξ_4= av(T_4) + ad(T_4) - 3 ξ_{34}= av(T_{34})+Max {2.5*ad(T_{34}),4}	Define: ξ_3=Min[320,av(T_3)+ 4*Max{sd(T_3),2}] ξ_{34}=Min[20,md(T_{34})+ 4*Max{sd(T_{34}),2}]
			Then, Confirm potential fires as real if: $T_3 > \xi_3$ and $T_{34} > \xi_{34}$	Then, Confirm potential fires as real if: $T_4 > \xi_4$ and $T_{34} > \xi_{34}$	Then, Confirm potential fires as real if: T_3>360 or [T_3>ξ_3 and T_{34}>ξ_{34}]
Filter hot surfaces	T_{34}≥14	T_{34}>15	Incorporated into fire detection	Incorporated into fire detection	Incorporated into fire detection
Filter clouds	T_4≥260	T_4>245	R_1+R_2≤1.2 and T_5≥265 and (R_1+R_2≤0.8 or T_5≥285)	*IGBP criteria applied here (no external cloud mask)*	*IGBP criteria applied here (no external cloud mask)*
Filter reflective surfaces	R_2≤0.22	R_1<0.25	R_2<0.20	R_2<0.25	
Filter sun glint		$\lvert R_1-R_2\rvert$>0.01			R_1≤0.3 or R_2≤0.3 or reflected sun angle ≥40°
Other detection criteria	T_{34}≥19 or T_{45}<4.1				
Post processing (not applied in this investigation)	Elimination of non-forest and isolated pixels	Quicklook inspection Max annual NDVI > 0			

R_1: reflectance in band 1 (0.66 μm); R_2: reflectance in band 2 (0.86 μm); T_3: brightness temperature in band 3 (3.75 or 3.95 μm for MODIS); T_4: brightness temperature in band 4 (10.8 μm); T_5: brightness temperature in band 5 (11.9 μm); T_{34}: T_3-T_4; T_{45}: T_4-T_5; av( ): mean; ad( ): mean absolute deviation; md( ): median, sd( ): standard deviation

considered to be cloud free. Note that some of the algorithms also include subjective tests (*e.g.*, visual inspection for fire smoke played an important role in eliminating false fires create by the ESA algorithm), which are not included here. Therefore, the results presented here may not be construed as the exact products generated by these algorithms, under the operational structure of the respective organizations using them.

To date, only the IGBP algorithm has been applied at a nearly global scale, including the majority of the Earth's biomes. The ESA algorithm was used mainly in the tropics including Africa, South America, and Australia. MODIS was developed for global operation. Note that the MODIS algorithm was not designed for use with AVHRR data *per se*, but the channels used in MODIS fire detection are sufficiently close to AVHRR channels. On the other hand, since the MODIS fire channel has a much higher saturation temperature and is shifted to a longer wavelength with a smaller contribution of sunlight, its performance as revealed here may be underestimated with respect to what could be realized with actual MODIS data. To adapt the algorithm to AVHRR data, the algorithm was modified somewhat. The modified algorithm is referred to as MODIS/AVHRR algorithm to differentiate it from the original MODIS algorithm that is actually applied to MODIS data. The algorithm of Giglio *et al.* (1999) has yet to be applied to global fire detection. The CCRS algorithm was designed for detecting Canadian boreal forest fires. The thresholds of the algorithm were derived from a fire database developed using satellite imagery alone (Li *et al.*, 2000c). Since no comparison was made against any ground-based fire data, the fire database can serve as ground-truth for validating the satellite fire product. The CCRS algorithm was also tested over areas in the Russian boreal forest and some temperate regions. During the fire season of 2000, the CCRS algorithm was used to generate daily fire products across both Canada and USA, just a few hours after all images covering these regions were received (ftp://ftp.ccrs.nrcan.gc.ca/ftp/ad/EMS/na_fires/). During the outbreak of fires that occurred in the western US states in the summer of 2000, such information played an important role for the Multi-Agency Coordination Group of the Northern Rockies Coordination Center to formulate its daily fire-fighting strategies (Wei-Min Hao, private communication). A preliminary assessment of the quality of the product by the US Forest Service showed similar performance compared to its application in Canada. Based on the confidence we have attained, the algorithm is being used to generate historical forest fire products across the continent of North America dating back to 1985 as a project of the NASA LCLUC program.

The main findings of the analysis are summarized below, while a detailed analysis will be presented in a separate paper (Ichoku *et al.*, 2000).

The spatial distribution of fire hot spots across Canada is similar among the algorithms under study, but the commission and omission errors differ significantly (Fig. 7). The CCRS algorithm was designed for boreal forest applications and thus provides superior overall performance in terms of trade-off between omission

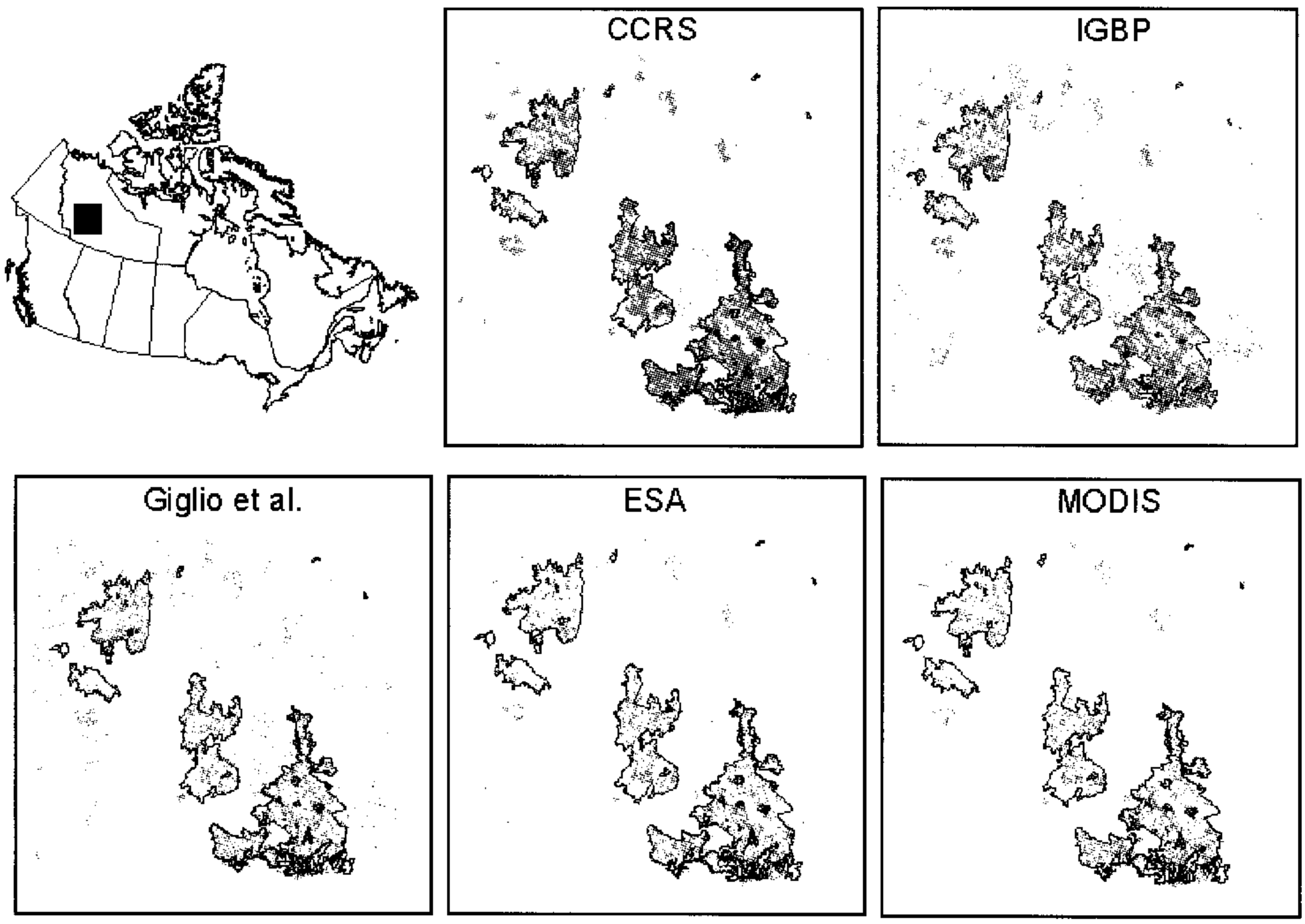

Fig. 7. Comparison of fire hot spots detected by the five algorithms against fire polygons obtained by Canadian forest agencies.

and commission errors (Fig. 7). Most of the hot spots detected by the CCRS algorithm fall within the CFS's fire polygons and some of those outside the polygons are verified to be real fires not mapped by provincial and territorial fire agencies (Fraser *et al.*, 2000). Fires missed by the CCRS algorithm are mainly obscured by cloud. The commission error is quite low, but not the lowest among the algorithms. The lowest commission error results from the MODIS/AVHRR algorithm, which occurs at the expense of missing a significant number of real fires. Other global algorithms also demonstrate trade-off between omission and commission errors. Similar to MODIS/AVHRR, the ESA algorithm is quite conservative, and also produces very few false fires. In contrast, the IGBP algorithm is too liberal with the highest level of commission error, but a low rate of omission error. The Giglio *et al.* algorithm results lie somewhere in between, with moderate omission and commission errors. In short, the results of fire detection with these leading algorithms are far from consistent in terms of numbers of fire pixels detected, but agree reasonably well in terms of the spatial pattern of fire distribution. Overall, no existing fire detection algorithm will likely perform optimally across a range of biomes and environments.

All algorithms suffer significant, but varying levels of commission error over the agricultural region in the Canadian western prairies (Fig. 8). Solar reflection from bare soil is thought to be the major cause, as many of the false alarms

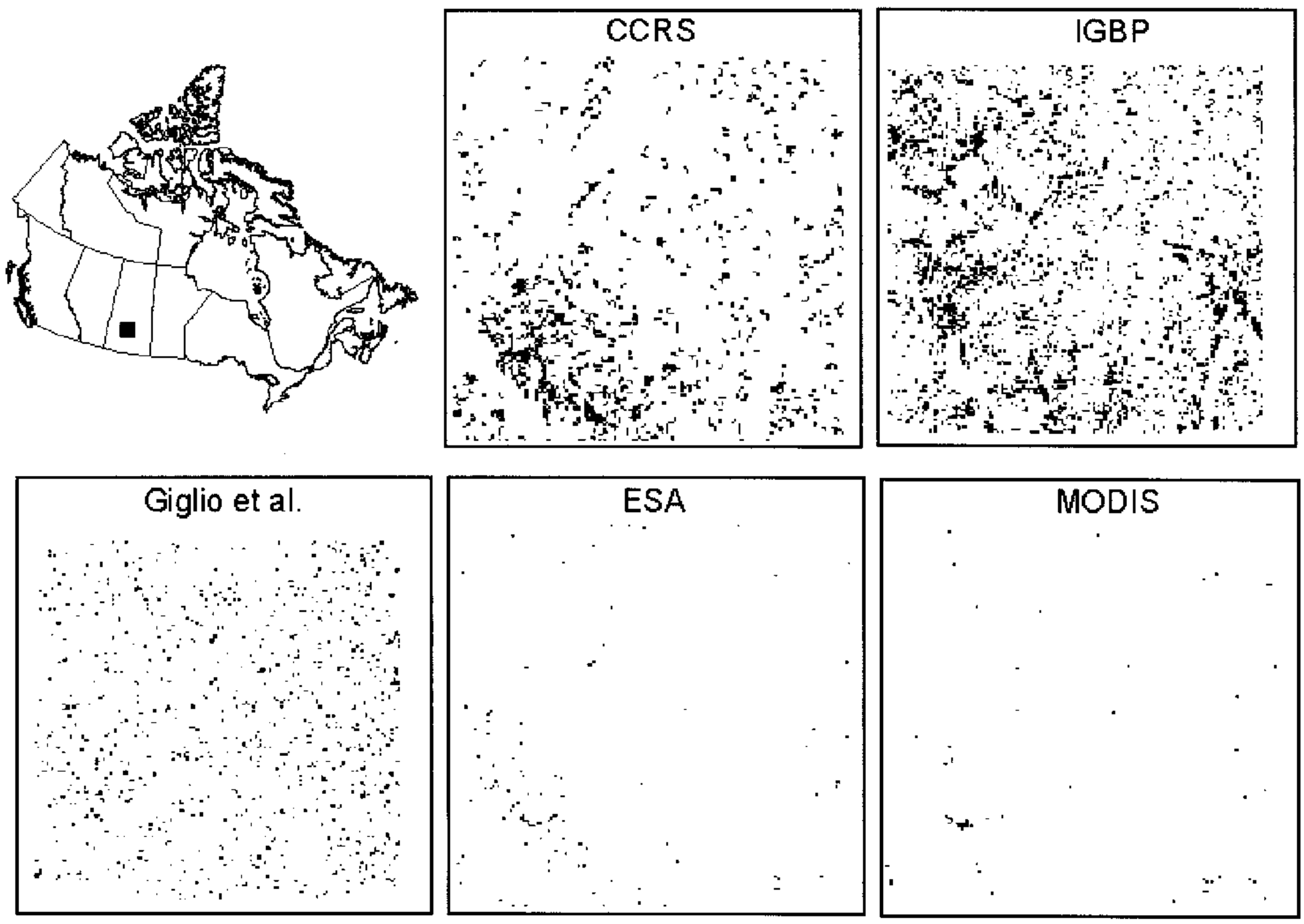

Fig. 8. Comparison of fire detection results by the five algorithms over the Canadian prairies.

occurred in late May and June when snow cover is gone but vegetation (mainly crops and grassland) has not greened up enough to cover the bare soil. Soil has much larger reflectance than green foliage, as observed by Salisbury and D'Aria (1994) who made extensive field observations for a large variety of terrestrial materials around the spectral region of AVHRR channel 3. The minimum, maximum, and mean values for many types of rocks, soil, and vegetation are computed from their tabulated data and plotted in Figure 9. Note that the dominant soil types in the western prairies are Mollisols and Aridisols whose albedo in channel 3 are up to ten times that of green foliage, which can easily cause confusion in all of the algorithms under consideration.

A correlation analysis was performed between the number of fire pixels detected daily by each of the five algorithms throughout Canada, regardless of whether they represent true or false fires, during the period 1st May to 31st October, 1995. The result is shown in Table 3. Overall, there are strong correlations between the number of pixels detected by the algorithms. ESA is very closely correlated with CCRS because they are both multi-channel fixed-threshold algorithms. All the contextual algorithms are correlated to the CCRS algorithm by approximately the same amount. On the other hand, the largest correlation exists between ESA and MODIS/AVHRR algorithms because of their strict fixed thresholds, and because the contextual thresholds used by MODIS/AVHRR are also strict for AVHRR data, and seldom applied in the cases observed.

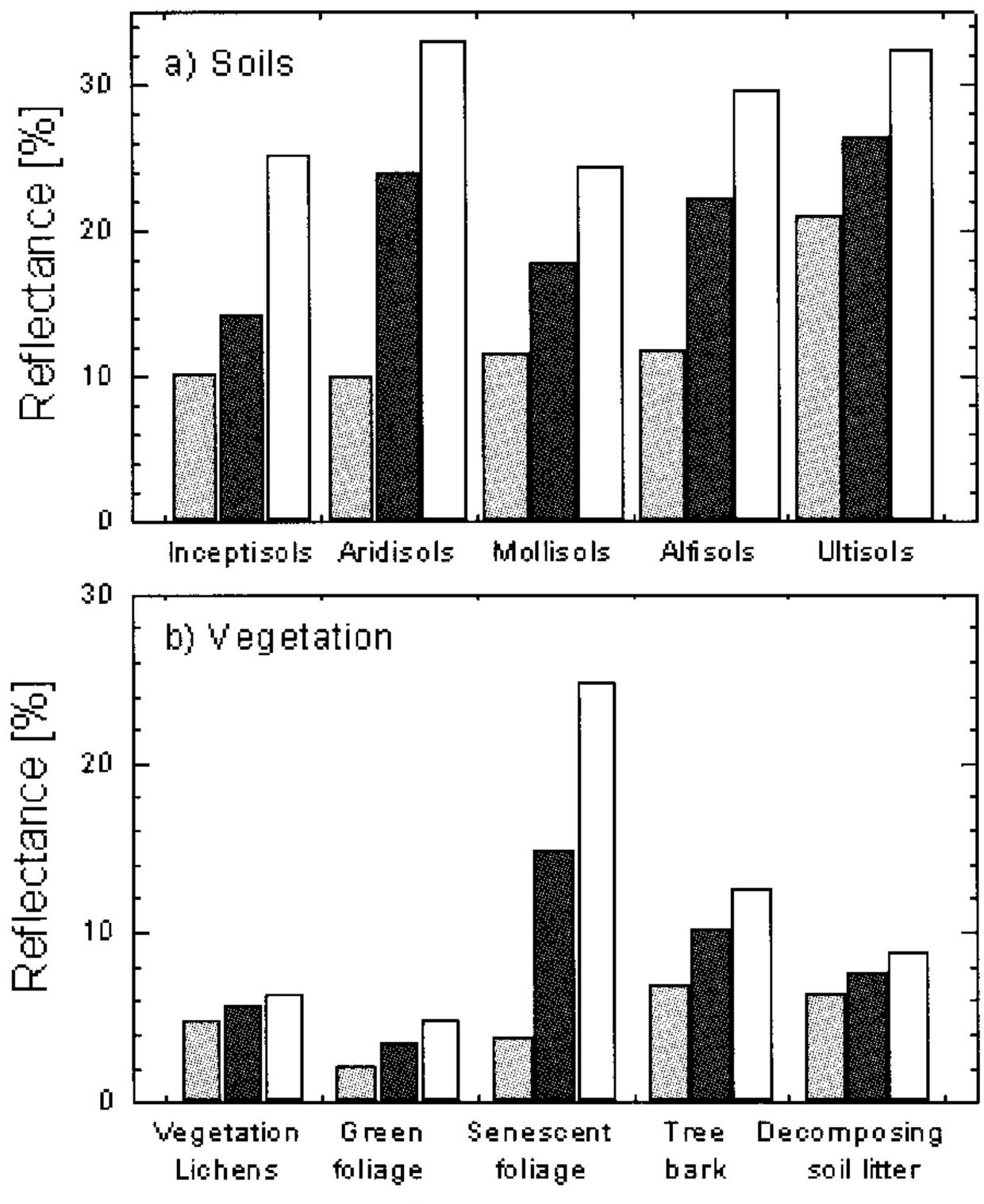

Fig. 9. Mean, minimum, and maximum values of reflectance in AVHRR channel 3 observed for many samples of soils (top) and vegetation (bottom) (reproduced from Salisbury and D'Aria, 1994).

Table 3. Correlations between the hot spots detected by the various algorithms

	CCRS	*ESA*	*GIGLIO*	*IGBP*	*MODIS/AVHRR*
CCRS	1.00				
ESA	0.91	1.00			
GIGLIO	0.80	0.81	1.00		
IGBP	0.82	0.70	0.80	1.00	
MODIS	0.81	0.94	0.77	0.62	1.00

It should be noted that a potential bias exists as a result of the validation method employed in this preliminary analysis (*i.e.*, comparison of cumulative hot spots to end-of-season burned area polygons). Specifically, any false alarms occurring within the CFS fire polygons will be misinterpreted as successfully detected active fire pixels, increasing the apparent detection rate. One potentially significant source of false alarms within these polygons are sub-regions burned earlier in the burning season, which are generally characterized by more exposed soil, less vegetation,

and the presence of ash. The resulting change in land cover may induce false alarms, especially among the contextual algorithms.

This phenomenon is clearly evident for the IGBP algorithm, which exhibited clusters of false alarms within several areas burned during the previous year (1994) (Li *et al.*, 2000b). The most prominent of these occur in the upper center and lower left of the forested area shown in Figure 7. It is likely that some of the 1995 hot spots were in fact burned (rather than burning) areas as well.

Recommendations for algorithm improvement

Although the findings discussed in the last section should be considered in the context of a regional application, it is safe to conclude that the performance of existing fire detection algorithms differs drastically. As a result, the quality of fire products generated from a single algorithm applied across various ecosystems may need considerable enhancement to meet the needs of user communities. To some extent, quality deficiencies originate from inherent technological limitations such as low frequency of satellite overpass, poor spatial resolution, sensor saturation, etc., that may not be resolved by means of research and development (R&D) into algorithm development. On the other hand, the potential capabilities of current space-borne observation technologies have not been fully explored and developed. In principle, the quality of fire products may be improved significantly by more R&D studies on the identification of algorithm limitations, and the innovation and improvement of algorithms. The drastic discrepancies among the algorithms evaluated above underscore the potential for algorithm improvement on a regional basis.

During the GOFC fire workshop, many discussions took place on the improvement of fire detection algorithms, some of which are outlined here. To improve an algorithm, its limitations must be identified first through extensive validation against ground-truth data sets as well as algorithm inter-comparison. Given the severe lack of ground-truth information, it is recommended that more field campaigns and operational air-borne fire monitoring exercises be conducted. Meanwhile, efforts are needed to identify and explore the utility of *all* existing ground-truth data sets. Validation using high-resolution satellite data sets, such as Landsat 7, is a sound alternative. As demonstrated above, algorithm inter-comparison is instrumental in identifying the range and source of uncertainties, which may be carried out for different ecosystems and sensors. The following specific recommendations will help solve some individual algorithm problems:

- setting thresholds based on land cover type, used to predict its albedo or emissivity;
- replacing threshold approaches by physical models;
- developing innovative algorithms to take advantage of multi-sensor capability offered by future satellite observations;
- exploring the utility of time series of images.

In developing and improving fire detection algorithms, the needs of different user groups should also be borne in mind. For the climate research community, the efficiency of running a detection algorithm is secondary to its accuracy, while for the fire management community, both accuracy and processing speed are very important. To date, more emphasis has been placed on the development of fire detection algorithm for the sake of climate change studies. Relatively less R&D efforts have been tailored to meeting the needs of a much larger user group, namely, the general public and fire management agencies. To satisfy these needs, fire detection algorithms are required to be *robust, fast, accurate, and automatic*. The algorithms should have very low rates of commission and omission errors, especially the latter. Little or no human supervision should be involved in running such algorithms.

Summary and concluding remarks

This paper presents an overview of fire detection algorithms designed primarily for use with AVHRR data, except one adapted for use with MODIS data. The emphasis of the review is placed on the physical principles, limitations, and potential improvement of the algorithms. Two major types of algorithms are dealt with in more detail, namely, the multi-channel threshold methods and the spatial contextual methods. In principle, the contextual methods are more versatile for application to a wide range of conditions than the fixed threshold approaches, but a threshold approach may provide more accurate results if it is specifically tailored for application to a particular region/biome. The most serious problems suffered by both types of algorithm are caused by the saturation of channel 3 and its contamination by solar reflection. Both these problems are anticipated to be resolved or lessened by the MODIS sensors due to the inclusion of a special fire channel (3.9 μm instead of 3.7 μm) that has a wider dynamic range and is less influenced by solar reflection. There remain several outstanding issues for AVHRR-based fire detection. The most challenging is to compensate for the contribution of solar radiation due to reflection from cloud and Earth's surfaces. The majority of the algorithms include cloud screening tests that are reasonably efficient in removing false alarms by clouds, but few algorithms are capable of eliminating false alarms caused by surface reflection. This leads to a high rate of commission error over bare land surfaces by the majority of fire detection algorithms. To overcome the problem, it is recommended to either screen out bright surfaces (in the channel 3 wavelengths) or to specify the threshold according to land cover types, or more precisely their expected radiance, without fire, as observed by the satellite.

Due to the importance of the T3-T4 test in multi-threshold detection algorithms, further insight was gained into the physical principles and limitations associated with this test. While it is often stated in the literature that the test helps distinguish fire hot spots from warm background, it is underlined here that the test only

works for thermally inhomogeneous pixels, regardless of the mean scene temperature itself. Although there are many factors affecting the T3-T4 difference, each of which was investigated, only thermal inhomogeneity has a positive and significant contribution to large differences in T3-T4 associated with fires. When there is temperature variability within a satellite's instantaneous field of view (IFOV) or pixel, radiance emitted from the burning portion of the IFOV is much larger in channel 3 than in channel 4, whereas their difference in radiance from the non-burned area is much smaller. The total radiance received by a sensor is a linear combination of separate radiances weighted by their areas. Therefore, when the total radiance is converted into brightness temperature using the non-linear Planck function, the difference between the two channels is proportional to the thermal inhomogeneity of the observed scene. Fortunately, most fire events are non-uniform at the AVHRR pixel size, making this test effective in removing the majority of the false fire alarms.

For the contextual algorithms, the selection of initial thresholds for identifying potential fire pixels is sensitive. An overly high setting leads to large omission errors, as the confirmation tests are only limited to potential fire pixels. On the other hand, an overly low setting introduces too much noise in determining the statistics for the background. Most of the contextual algorithms employed fixed and identical thresholds to identify potential fire pixels and the background non-fire pixels. Considering the different functions and consequences of threshold settings, it is recommended that more liberal thresholds be used to identify potential fire pixels and more conservative thresholds be used to calculate non-fire background statistics. Since the severity of a fire varies considerably with fuel type, fuel amount, and weather conditions, the thresholds should also be contingent upon these variables. As a first approximation, one may use different thresholds over different land cover types in different seasons, or set the threshold as a function of a vegetation index.

While many fire detection algorithms have been employed to generate fire products, the products still encompass much shorter time periods and smaller geographic areas than are potentially available from the satellite data archive (Gutman *et al.*, this volume). For example, the global IGBP fire product was generated for only 20 months (1992-1993). An operational near-real time fire product providing global coverage became available only recently from the World Fire Web network. Longer-term operational fire products are available in very limited geographic areas such as in Brazil and Canada (seven years). However, increasing efforts are being made to produce much more comprehensive fire products from AVHRR. NOAA's archive of 1-km AVHRR data dating back to 1985 is being exploited to generate a historical fire data base across North America's forests. Many efforts are also being undertaken in other countries, especially in Europe, to generate both near real-time and historical fire products. It is envisioned that, before long, we will encounter multiple fire products over the same region/ period. Evaluation of the quality of these products becomes a more challenging

issue than generating them. The evaluation is tied directly to the quality of fire detection algorithm.

Acknowledgments

The views and comments expressed in this paper originated not only from the authors of the article, but also from the fire community at large, especially the participants of the GOFC Fire Workshop held at the Joint Research Centre in Italy 1999. We are particularly grateful to F. Ahern, C. Justice, and J.-M. Grégoire, for their leadership and dedication to the GOFC fire program, which made this publication possible.

References

Ahern F., A.C. Janetos, and E. Langham. (1998), Global Observation of Forest Cover: One Component of CEOS' Integrated Global Observing Strategy, *Proceedings of the 27th International Symposium on Remote Sensing of Environment*, Tromsø, Norway, June 8-12.

Anderson, G.P., F.X. Kneizys, J.H. Chetwynd, L.S. Rothman, M.L. Hoke, A. Berk, L.S. Bernstein, P.K. Acharya, H.E. Snell, E. Mlawer, S.A. Clough, J. Wang, S.-C. Lee, H.E. Revercomb, T. Yokota, L.M. Kimball, E.P. Shettle, L.W. Abreu, and J.E. Selby. (1996), Reviewing atmospheric radiative transfer modeling: new developments in high- and moderate-resolution FASCODE/FASE and MODTRAN, *Proceedings SPIE* 2830:82-93.

Arino, O., and J.M. Mellinotte. (1998), The 1993 Africa fire map, *International Journal of Remote Sensing*, 19:2,019-2,023.

Arino, O., and J.-M. Rosaz. (1999), 1997 and 1998 World ATSR Fire Atlas using ERS-2 ATSR-2 Data, *Proceedings of the Joint Fire Science Conference*, Boise, 15-17 June.

Barbosa, P.M., J.-M. Grégoire, and J.M.C. Pereira. (1999), An algorithm for extracting burned areas from time series of AVHRR GAC data applied at continental scale, *Remote Sensing of the Environment*, 69:253-263.

Belward, A.S., P.J. Kennedy, and J.-M. Grégoire. (1994), The limitation and potential of AVHRR GAC data for continental scale fire studies, *International Journal of Remote Sensing*, 15:2,215-2,234.

Belward, A.S., J.-M. Grégoire, G. D'Souza, S. Trigg, M. Trigg, M. Hawkes, J.-M. Serca, J.-L. Tireford, J.-M. Charlot, R. Vuattoux. (1993), In situ, real time fire detection using NOAA/AVHRR data, *Proceedings of the VI AVHRR Data User's Meeting, Belgirate*, Italy, 29th June–2nd July, published by EUMETSAT, Darmstadt, Germany, EUM P 12, ISSN 10159576, pp. 333-339.

Cahoon, D.R., Jr., J.S. Levine, P. Minnis, G.M. Tennille, T. W. Yip, P.W. Heck, and B.J. Stocks. (1991), The great Chinese dire of 1987: A view from space, in *Global Biomass Burning: Atmospheric, Climate, and Biospheric Implications* (J.S. Levine, Ed.), MIT Press, Cambridge, MA, pp. 61-66.

Cahoon, D.R., Jr., B.J. Stocks, J.S. Levine, W.R. Cofer III, and K.P. O'Neill. (1992), Seasonal distribution of African savanna fires, *Nature*, 359:812-815.

Cahoon, D.R., Jr., B.J. Stocks, J.S. Levine, W.R. Cofer III, and J.M. Pierson. (1994), Satellite analysis of the severe 1987 forest fires in northern China and southeastern Siberia, *Journal of Geophysical Research*, 99:18,627-18,638.

Chu, A., Y.J. Kaufman, L.A. Remer, and B.N. Holben. (1998), Remote sensing of smoke from MODIS Airborne Simulator During SCAR-B Experiment, *Journal of Geophysical Research*, 103:31,979-31,988.

Chuvieco, E., and R.G. Congalton. (1988), Mapping and inventory of forest fires from digital processing of TM data, *Geocarto International*, 3:41-53.

Chuvieco, E., and M.P. Martin. (1994), A simple method for fire growth monitoring using AVHRR channel 3 data, *International Journal of Remote Sensing*, 15:3,141-3,146.

Coakley, Jr, J.A. and F.P. Bretherton. (1982), Cloud cover from high-resolution scanner data: detecting and allowing for partially filled fields of view, *Journal of Geophysical Research*, 87:4,917-4,932.

Crutzen, P.J., L.E. Heidt, J.P. Krasnec, W.H. Pollock, and W. Seiler. (1979), Biomass burning as a source of atmospheric gases, CO, H_2O, N_2O, NO, CH3CL and COS, *Nature*, 282:253-256.

Crutzen, P.J., and M.O. Andreae. (1990), Biomass burning in the tropics: Impact on atmospheric chemistry and biogeochemical cycle, *Science*, 250:1669-1678.

Dozier, J. (1981), A method for satellite identification of surface temperature fields of subpixel resolution, *Remote Sensing of the Environment*, 11:221-229.

Dwyer, E., J.-M. Grégoire, and J.-P. Malingreau. (1998), A global analysis of vegetation fires using satellite images: Spatial and temporal dynamics, *Ambio*, 27:175-181.

Eva, H., and S. Flasse. (1996), Contextual and multiple-threshold algorithms for regional active fire detection with AVHRR data, *Remote Sensing Revue*, 14:333-351.

Eva, H.D., and E. Lambin. (1998), Burnt area mapping in central Africa using AATSR data, *International Journal of Remote Sensing*, 18:3473-3497.

Flannigan, M.D., and T.H. Vonder Haar. (1986), Forest fire monitoring using NOAA satellite AVHRR, *Canadian Journal Forest Research*, 16:975-982.

Flasse, S.P., and P. Ceccato. (1996), A contextual algorithm for AVHRR fire detection, *International Journal Remote Sensing*, 17:419-424.

Franca, J.R, J.M. Brustet, and J. Fontan. (1995), Multispectral remote sensing of biomass burning in West Africa, *Journal of Atmos. Chem.*, 22:81-110.

Fraser, R.H., Z. Li, and J. Cihlar. (2000), Hotspot and NDVI Differencing Synergy (HANDS): a new technique for burned area mapping over boreal forest, *Remote Sensing of the Environment*, 74:362-376.

Giglio, L., J.D. Kendall, and C.O. Justice. (1999), Evaluation of global fire detection using simulated AVHRR infrared data, *International Journal of Remote Sensing*, 20:1947-1985.

Hovis, W.A. Jr. (1966), Infrared spectral reflectance of some common minerals, *Applied Optics*, 5:245-248.

Ichoku, C., Y. Kaufman, L. Giglio, Z. Li, R. Fraser, J.-Z. Jin, and B. Park. (2000), Comparative analysis of daytime fire detection algorithms using AVHRR data for the 1995 fire season in Canada: Perspective for MODIS. In preparation.

Inoue, T. (1987), A cloud type classification with NOAA-7 split-window measurements, *Journal of Geophysical Research*, 92:3,991-4,000.

Justice, C., J.P. Malingreau, and A.W. Setzer. (1993), Remote sensing of fires: Potential and limitations, in *Fire in the Environment* (P.J. Crutzen and J.G. Goldammer, Eds.), pp. 77-88. John Wiley & Sons, Chicester

Justice, C.O., and J.P. Malingreau (editors). (1993), *The IGBP-DIS Satellite Fire Detection Algorithm Workshop Technical Report*, IGBP-DIS Working Paper 9, NASA/GSFC, Greenbelt, MD, February.

Justice, C., and J.P. Malingreau (editors). (1996), *Report of the IGBP-DIS fire algorithm workshop 2*, IGBP-DIS working paper 14, Ispra, Italy, October 1995.

Justice, C.O., J.D. Kendall, P.R. Dowty, and R.J. Scholes. (1996), Satellite remote sensing of fires during the SAFARI campaign using NOAA advanced very high resolution radiometer data, *Journal of Geophysical Research*, 101:23,851-23,863.

Justice, C.O., and J.P. Malingreau (editors). (1993), *The IGBP-DIS Satellite Fire Detection Algorithm Workshop Technical Report*, IGBP-DIS Working Paper 9, NASA/GSFC, Greenbelt, Maryland, USA, February.

Kasischke, E.S., N.H.F. French, P. Harrell, N. Christensen, Jr., S.L. Ustin, and D. Barry. (1993), Monitoring of wildfires in boreal forests using large area AVHRR NDVI composite image data, *Remote Sensing of the Environment*, 45:61-71.

Kaufman, Y.J. and R.S. Fraser. (1997). The effect of smoke particles on clouds and climate forcing, *Science*, 277:1,636-1,639.

Kaufman, Y.J., C. Justice, L. Flynn, J. Kendall, E. Prins, D.E. Ward, P. Menzel, and A. Setzer. (1998a), Potential global fire monitoring from EOS-MODIS, *Journal of Geophysical Research*, 103:32,215-32,238.

Kaufman, Y.J., R.G. Kleidman, and M.D. King. (1998b), SCAR-B Fires in the Tropics: Properties and their remote sensing from EOS-MODIS, *Journal of Geophysical Research*, 103:31,955-31,969.

Kaufman, Y.J., D. Tanré, L. Remer, E. Vermote, A. Chu, and B.N. Holben. (1997), Remote sensing of tropospheric aerosol from EOS-MODIS over the land using dark targets and dynamic aerosol models, *Journal of Geophysical Research*, 102:17,051-17,067.

Kaufman, Y.J., and L. Remer. (1994), Detection of forests using mid-IR reflectance: An application for aerosol studies, *IEEE Journal of Geoscience and Remote Sensing*, 32:672-683.

Kaufman, Y.J., D. Tanre, and D.E. Ward. (1994), Remote sensing of biomass burning in the Amazon, *Remote Sensing Revue*, 10:51-90.

Kaufman, Y.J., C.J. Tucker, and I. Fung. (1990), Remote sensing of biomass burning in the tropics, *Journal of Geophysical Research*, 95:9,927-9,939.

Kennedy, P.J., A.S. Belward, and J.-M. Grégoire. (1994), An improved approach to fire monitoring in West Africa using AVHRR data, *International Journal of Remote Sensing*, 15:2,235-2,255.

Langaas S. (1992), Temporal and spatial distribution of Savannah fires in Senegal and the Gambia, West Africa, 1989-90, derived from multi-temporal AVHRR night images, *International Journal of Wildland Fire*, 2:21-36.

Langaas S. (1993), A parameterised bispectral model for savanna fire detection using AVHRR night images, *International Journal of Remote Sensing*, 14:2,245-2,262.

Lee, T.M., and P.M. Tag. (1990), Improved detection of hotspots using the AVHRR 3.7 μm channel, *Bulletin of the American Meteorological Society*, 71:1,722-1,730.

Li, Z., H. Barker, and L. Moreau. (1995), The variable effect of clouds on atmospheric absorption of solar radiation, *Nature*, 376, 486-490.

Li, Z. (1998), Influence of absorbing aerosols on the solar surface radiation budget, *Journal of Climate*, 11:5-17.

Li, Z., J. Cihlar, L. Moreau, F. Huang, and B. Lee. (1997), Monitoring fire activities in the boreal ecosystem, *Journal of Geophysical Research*, 102:29,611-29,624.

Li, Z., A. Khananian, and R. Fraser. (2000a), Detecting smoke from boreal forest fires using neural network and threshold approaches applied to AVHRR imagery, *IEEE Tran. Geoscience and Remote Sensing*, revised.

Li, Z., S. Nadon, J. Cihlar, and B. Stocks. (2000b), Satellite mapping of Canadian boreal forest fires: Evaluation and comparison of algorithms, *International Journal of Remote Sensing*, 21:3,071-3,082.

Li, Z., S. Nadon, and J. Cihlar. (2000c), Satellite detection of Canadian boreal forest fires: Development and application of an algorithm, *International Journal of Remote Sensing*, 21:3,057-3,069.

Malingreau, J.P. (1990), The contribution of remote sensing to the global monitoring of fires in tropical and sub-tropical ecosystems, in *Fire in the Tropical Biota* (J.G. Goldammer, Ed.), Berlin: Springer-Verlag, pp. 337-370.

Malingreau J.P., and C.J. Tucker. (1988), Large scale deforestation in the south-eastern Amazon basin, *Ambio*, 17:49-55.

Malingreau, J.P., and C.O. Justice, (editors). (1997), *The IGBP-DIS Satellite Fire Detection Algorithm Workshop Technical Report*, IGBP-DIS Working Paper 17, NASA/GSFC, Greenbelt, Maryland, USA, February.

Martin, P., P. Ceccato, S. Flasse, and I. Downey. (1999), Fire detection and fire growth monitoring using satellite data, in *Remote Sensing of Large Wildfires in the European Mediterranean Basin* (E. Chuvieco, Ed.), Springer-Verlag Berlin/Heidelberg 3-540-65767-3, XII, pp. 212.

Matson, M., G. Stephens, and J. Robinson. (1987), Fire detection using data from the NOAA-N satellites, *International Journal of Remote Sensing*, 8:961-970.

Menzel, W.P., E.C. Cutrim, and E.M. Prins. (1991), Geostationary satellite estimation of biomass burning in Amazonia during BASE-A, in *Global Biomass Burning* (J.S. Levine, Ed), MIT Press, Cambridge, MA, pp. 41-46.

Muirhead, K. and A. Cracknell. (1985), Straw burning over Great Britain detected by AVHRR, *International Journal of Remote Sensing*, 6:827-833.

Pereira, M.C., and A.W. Setzer. (1993), Spectral characteristics of deforestation fires in NOAA/AVHH images, *International Journal of Remote Sensing*, 14:583-597.

Pereira, J.M.C. (1999), A comparative evaluation of NOAA/AVHRR vegetation indexes for burned surface detection and mapping, *IEEE Trans. Geoscience and Remote Sensing*, 37:217-226.

Prins, E.M., and W.P. Menzel. (1994), Trends in South American biomasss burning detected with the GOES VISSR radiometer atmospheric sounder from 1983 to 1991, *Journal of Geophysical Research*, 99:16,719-16,735.

Prins, E.M., and W.P. Menzel. (1992), Geostationary satellite detection of biomass burning in South America, *International Journal of Remote Sensing,* 13:2,783-2,799.

Rauste, Y., E. Herland, H. Frelander, K. Soini, T. Kuoremaki, and A. Ruokari. (1997), Satellite-based forest fire detection for fire control in boreal forests, *International Journal Remote Sensing*, 18:2,641-2,656.

Razafimpanilo, H., R. Frouin, S.F. Iacobellis, and R.C.J. Somerville. (1995), Methodology for estimating burned area from AVHRR reflectance data, *Remote Sensing of the Environment*, 54:273-289.

Robinson, J.M. (1991), Fire from space: Global fire evaluation using infrared remote sensing, *International Journal of Remote Sensing*, 12:3-24.

Salisbury, J.W., and D.M. D'Aria. (1994), Emissivity of terrestrial materials in the 3-5 ìm atmospheric window, *Remote Sensing of the Environment*, 47:345-361.

Setzer A.W., and M.C. Pereira. (1991a), Operational detection of fires in Brazil with NOAA-AVHRR, *24th Symposium on Remote Sensing of the Environment*, ERIM, Rio de Janeiro, Brazil, May.

Setzer, A.W., and M.C. Pereira. (1991b), Amazonian biomass burnings in 1987 and an estimate of their tropospheric emission, *Ambio*, 20:19-22.

Setzer, A.W., and M.C. Pereira. (1992), Operational detection of fires in Brazil with NOAA-AVHRR., Rio de Janeiro, *Proceedings of the 24th International Symposium on Remote Sensing of the Environment*, ERIM, pp. 469-482.

Setzer, A.W., M.C. Pereira, Jr., and A.C. Pereira. (1994), Satellite studies of biomass burning in Amazonia: Some practical aspects, *Remote Sensing Revue*, 10:91-103.

Setzer, A.W., and J.P. Malingreau. (1996), AVHRR monitoring of vegetation fires in the tropics: Toward the development of a global product, in *Biomass Burning and Global Change* (J.S. Levine, Ed.), MIT Press, Cambridge, MA, and London, pp. 25-39.

Suits, G.H. (1989), Natural sources, in *The Infrared Handbook* (W.L. Wolfe and G.J. Zissis, Eds.), Ann Arbor, MI, E.R.I.M., pp. 3.1-3.154.

Vines, R.G. (1981), Physics and chemistry of rural fires, in *Fire and the Australian Biota* (A.M. Gill, R. H. Groves and I.R. Noble, Eds.), Canberra: Australian Academy of Science, pp. 129-151.